Film Characterization and Evaluation of Process Performance for the Modified Electron Beam Resist

Fu-Hsiang Ko[a], Jyh-Hua Ting[a], Cheng-Tung Chou[b], Li-Tung Hsiao[b], Tiao-Yuan Huang[a] and Bau-Tong Dai[a]

[a]National Nano Device Laboratories, National Chiao Tung University, Hsinchu 300, Taiwan
[b]Department of Chemical Engineering, National Central University, Chung-Li, Taoyuan 320, Taiwan

ABSTRACT

The modification of the electron beam resist by spiking with various amounts of poly(styrene-co-maleic anhydride) copolymer is performed. The characterization of resist solutions by gel permeation chromatography (GPC) and viscosity measurement reveals the main polymer chain in the resist is unchangeable, irrespective of the amount of modification. In addition, the spiking copolymer exists in original form. The viscosity of the resist increases with the amount of spiking polymer. Our thermal analysis results show that the resists are mainly decomposed in two regions (280 and 544℃). The mass loss at 280℃ is significant higher than at 544℃. The spectra of Fourier transform infrared red (FTIR) spectrometer indicate the extent of carbonate group decomposition decreases with temperature for resists. The plasma etching experiment indicates the promotion of etching resistance of the resist film is due to modification, while the resolution, sensitivity and contrast are not degraded. Owing to the polymer aggregation effect, the stripping performance of the resist film can achieve better after copolymer modification.

Key words: resist modification; resist characterization; thermal analysis; resist stripping performance

1. INTRODUCTION

The next generation ultralarge scale integration circuits (ULSIs) will require deep submicron feature size due to the increasing demand for high-density memories and high-speed logic devices.[1] The optical illumination technique has face resolution limit, and numerous resolution enhancement techniques (RETs) such as phase-shifting mask (PSM), off-axial illumination (OAI), optical proximity correction (OPC) and custom illumination aperture (CIA) have been proposed to extend the capability of optical technique.[2-7] In the alternate ways, the anti-reflective coating (ARC), silylation technique and bilayer resist have also been used in optical lithography to improve the manufacturing capability.[8-10] However, the resultant cost is extreme high for the promotion of resolution and process reliability.

Compared with the optical technique, electron can be focused in very fine area. Like photons, electrons possess particle and wavelike properties, but their wavelength is 4 to 5 orders of magnitude shorter than the wavelength of ultraviolet illumination used in optical lithography. If the wafer surface is coated with a radiation-sensitivity electron-beam resist, the electron beam can be used to write patterns with very high resolution. Based on these reasons, the electron techniques such as direct-writing, shaped beam exposure, and electron projection (combining of shaped beam and projection) have become the candidate for future lithography.[11-13]

In the electron beam lithography, the exposure system and the process are still need to be improved. Due to the lower throughput of the present electron beam machine, the electron lithography can not compete with the optical lithography for mass production. In the process consideration, the problems[14-16] of electron proximity and accumulation effects, and the unfavorable etching resistance of resist also restrict the applicability of electron beam technique. Literatures[17-19] have been reported that the baking condition, developer type and the edge roughness in resist pattern can deeply influence the process resolution and sensitivity for electron beam lithography. Therefore, the evaluation of process window and capability on such factors is of prime importance.

The etching resistance of resist is strongly dependent on the resist structure. However, little has been reported regarding the effect of polymer modification on the etching resistance. This could be attributed to the fact that their actual components in resist are unclear, therefore structure discrimination is rather difficult. The polymer constituent in the resist after development and hardbaking must be able to withstand the plasma etching and ion implantation. Ishii and coworkers[16] use the fullerene (i.e., C_{60}) to modify the electron beam resists. They find the pattern contrast, etching resistance and postexposure delay can be improved by spiking fullerene. Our previous report[20] uses the poly(4-vinylphenol) polymer to modify the optical resist, this modification is beneficial for the thermal stability, resolution and reducing swing effect.

In *Advances in Resist Technology and Processing XVII*, Francis M. Houlihan, Editor, Proceedings of SPIE Vol. 3999 (2000) • 0277-786X/00/$15.00

Downloaded From: http://proceedings.spiedigitallibrary.org/ on 04/28/2014 Terms of Use: http://spiedl.org/terms

This study attempts to investigate the modification of the electron beam resist by spiking various amounts of copolymer, i.e., poly(styrene-co-maleic anhydride). The molecular weight, viscosity and thermal stability are evaluated with various instrumental methods. The etching durability and the lithographic behavior are also studied. In addition, the novel thermal desorption system – atmospheric pressure ionization mass spectrometry (TDS-APIMS) method is developed and applied to study the effect of copolymer modification on resist stripping.

2. EXPERIMENTAL

2.1 Materials

The positive electron beam resist (i.e., ZEP520) used in this study was purchased from Nippon Zeon Company (Tokyo, Japan). The average molecular weight of the resist is about 54000 Da. Modification of resists were prepared by adding 0, 0.5 and 1 g of poly(styrene-co-maleic anhydride) copolymer (M_n about 1900 Da, Aldrich, WI, USA) into 50 mL resist solution, respectively, and then stirred overnight in a dark room. These respective resists were named resists A (i.e., non-modified control), B and C in this work. Tetrahydrofuran (THF) solvent obtained from E. Merck (Darmstadt, Germany) was used as the eluent for gel permeation chromatography (GPC) experiment.

The relationship between the molecular weight (MW) and retention time for the gel permeation column was calibrated by monitoring the retention time of several pure polystyrene standards including MW of 38991, 20298, 9658, 4782, 2046 and 603 Da, respectively. These standards were obtained from Alltech Associates (IL, USA). The total exclusion volume of the GPC system was estimated by using the polyethylene oxide (MW, 1390 KDa). All the polymer standard solutions were prepared with THF solvent and then filtered through the 0.45μm membrane before use.

2.2 Instrumentation and Thermal Analysis

The GPC system consisted of a dual-piston solvent-delivery pump (Hitachi, Model L-7100, Tokyo, Japan) equipped with an automatic sample injector (Rheodyne 9125, Cotati, CA). The identification of MW distribution of resist was performed by separating the sample with four columns used in series, namely LiChrogel^R PS 4 (in the range 100-5K Da), PS 20 (in the ange 100-20K Da), PS 40 (in the range 100-40K Da) and PS 400 (in the range 500-400K Da). The effluent from the column system was subsequently detected with ultraviolet detector (Hitachi, Model-4250).

Film thickness was measured using either an Nanospec optical film thickness monitor manufactured by Nanometrics Incorporated (CA, USA) or a Model 1200 n&k analyzer (n&k Technology, CA, USA).

For evaluation of the structure variation after thermal treatment, the Fourier transform infrared red (FTIR, Bio-Rad, Model FTS-40, MA) spectrometer was used. The resist samples, after coating onto the wafer (the procedure see below), was measured in the range 4000 and 400cm^{-1}.

For preparation of sample on thermogravimetric analysis (TGA), the resist samples (5mL) were put on the aluminum foil and then bake at 150℃ on a hotplate for ten minutes. After cooling, the resist film was scrubbed from the foil and put into the ceramic sample holder of the thermal analyzer (Seiko Model SSC-5200, Chiba, Japan). The approximate sample weight used for thermal analysis was 5 to 10mg. The heating rate was 10℃/min, and the heating cycle was achieved from room temperature to 900℃ for the TGA analysis.

2.3 Lithography Process

Wafers, 6-inch in diameter, were first primed with hexamethyldisilazane (Merck). They were then coated with resists at spin rate of 4500rpm for 20sec. After softbaking (180℃, 120sec), wafers were sent to characterization. In order to investigate the variation of resolution, sensitivity and contrast of the resists, samples were irradiated on the high-resolution vector-scan electron beam machine, EBML 300, made by Leica Cambridge company. The beam current was 300pA and the accelerating voltage was 40KV. Once exposure the resists were again baking at 110℃ for 120sec. Finally, wafers were developed with organic solvent (MD-G, from Nippon Zeon), and then hardbaking (120℃, 120sec). The resist patterns were examined with the field emission scanning electron microscopy (Hitachi S-4000).

2.4 Resist Stripping after Plasma Etching and Ion Implantation

For testing the resist stripping, the wafers coated with the resist were transferred to the reactive ion etcher (Tokyo Electron Limited, Model TE 5000, Tokyo) and middle current ion implantation (Varian E200). The etcher was composed with a 380 KHz RF generator, applying both on the upper and lower electrodes with power split mode. The respective

Downloaded From: http://proceedings.spiedigitallibrary.org/ on 04/28/2014 Terms of Use: http://spiedl.org/terms

temperatures are 20, -13 and 40℃ for the upper and lower electrodes, and the chamber. The operating conditions of the etcher were listed in Table 1. The ion implantation can operate in the energy range 5 to 200KV. The dose of the machine can be adjusted during 10^{11} to 10^{16} ions/cm^2. In this study, the As^+ from AsH_3 gas was implanted at the dose of $5x10^{15}$ions/cm^2 into the resist. After plasma etching or ion implantation, the resist was subsequent stripping with ozone ashing and SPM clean (the mixture of sulfuric acid and hydrogen peroxide). Then, the sample are analyzed with TDS-APIMS (Model UG-21 and 400P, Hitachi Tokyo Electronic) in the temperature range 25 to 800℃. The purge gas was argon, and the temperature ramping rate was 100℃/min.

3. RESULTS AND DISCUSSION

3.1 Characterization of Modified Electron Beam Resist

In this study, the molecular weight and viscosity of resist solution after spiking with various amounts of poly(styrene-co-maleic anhydride) copolymer are analysis. Prior to determining the molecular weight (MW) of the resists, the MW calibration curve needs to be established based on the polymer standards as mentioned in the experimental section. The MW range of the in series four columns is achieved by plotting log(MW) versus elution time. It exhibits linear elution behavior with the MW calibration curve of $y = -0.2219x + 8.3404$ and correlation coefficient of 0.996. The MW of each resist sample can be obtained from the elution time by using the MW calibration curve.

Figure 1 shows the chromatogram for the separation of species with various MWs in resist C. It can be seen from the chromatogram that there are totally seven peaks to be eluted out. By using the MW calibration curve, these peaks represent the MWs of 52897, 1824, 839, 538, 305, 125 and 67 Da, respectively. The 52897 Da belongs to the polymer chain in resist A, and very close to the average molecular weight (54000 Da) provided by the vendor. The MW of 1824 Da is explained in the following. The other peaks belong to the additive and solvent of the resist. Although the chromatograms for resists A and B are not shown here, their chromatograms are similar with resist A. The only difference for the chromatograms is found at the peak of 1824 Da. The peak only appears in resists B and C, and comes from the spiking polymer. From the prediction of GPC analysis, the spiking copolymer has no interaction with the original resist. These resists are also subjected to the viscosity analysis. The respective viscosity for resist solutions A, B and C is 22, 24.3 and 26.4cP. It can be found that the viscosity shows very good linear relationship with the amount of spiking copolymer.

After testing the MW distribution and viscosity for various resist solutions, the resists are coated onto the silicon substrate for thickness, FTIR and thermal analysis. Figure 2 illustrates the effect of spin rate on the resist thickness. It can be found that the resist thickness gradually decreases with spin rate. In the same spin rate, the thickness increases with the amount of spiking copolymer. This result is attributed to the increase of viscosity for resist solution. Literature[11-12] has been proposed the following semi-empirical equation to describe the effect of molecular weight (η), resist polymer concentration (C), and spin rate (ω) on the coating thickness (t).

$$t = \frac{KC^{\beta}\eta^{\gamma}}{\omega^{\alpha}}$$

The K represents the overall constant, while coefficients α, β and γ can be determined from the experiment. The α, β and γ are important coefficient to describe the effect of molecular weight, resist polymer concentration and spin rate. In this study, the respective spin rate coefficients (α) obtained from the slope of Figure 2 are 0.47, 0.55 and 0.67 for resists A, B and C. This observation indicates the polymer modification can increase the spin rate coefficient.

The ZEP520 electron beam resist is composed of two main components, i.e., copolymer and solvent. The copolymer, of which the structure is shown in Figure 3, consists of α-chloromethacrylate and α-methylstyrene. The solvent is ortho-dichlorobenzene. As the electron beam imposes on the resist layer, the carbonate group in resist polymer chain becomes scission. Subsequently, the developer can dissolve the scission polymer with lower molecular weight.

For characterization of modified resist, FTIR spectrum is a simple method for revealing the structure variation. Figure 4 depicts the various FTIR spectra for resists. The peaks appeared in 1730 and 1755cm^{-1} for resists belong to the vibration of carbonyl group. In addition, the peak at 1780cm^{-1} is only found for resists B and C. It can be seen the peak height at 1780cm^{-1} increases with the amount of spiking copolymer. This vibration mode can be assigned to the carbonyl group in modifier. Beside this, other peaks are appeared in the same position. This finding reveals there is no interaction between the resist A and the spiking copolymer.

3.2 Thermal Analysis

In lithography, the processes of resist coating, softbaking, exposure, post exposure baking, development and

Downloaded From: http://proceedings.spiedigitallibrary.org/ on 04/28/2014 Terms of Use: http://spiedl.org/terms

hardbaking should be applied to define the pattern. The thermal window of the baking process is strongly dependent on the resist structure. Generally, positive resist shows endothermic reaction due to thermal-induced polymer chain scission, while negative resist exhibits exothermic reaction due to thermal-induced crosslinking. The thermal stability of the resist can be evaluated by TGA method.

Figure 5 shows the effect of baking temperature on the mass change, and the plotting of derivative TGA curve against temperature for resist A. It can be seen that the mass losses of the sample increase with temperature. The tendency of derivative thermogravimetry indicates the mass losses appear at two main regions (i.e., 280 and 544℃). Despite the TGA curves for resists B and C are not shown here, they has the similar behavior as resist A. Table 2 indicates the decomposition temperature and the percentage of mass losses from TGA curve. It can be found that the mass losses of these resists of first decomposition temperature are in the same. However, the mass losses in second decomposition temperature decrease after copolymer spiking. This observation indicates the copolymer modification can enhance the thermal stability. Interestingly up to 600℃ baking, there still exists about 0.5 to 0.9% of residual, indicating the formation of refractory residual at higher temperature.

In order to resolve the thermal decomposition was come from which constituent in the resist. These resists, respective baking at 140, 180, 220, 260 and 300℃, are measured with FTIR. In the previous section, the characteristic behavior of FTIR spectra has been discussed. For the ease of understanding the baking effect, the spectra of resist A can be used as an example. From Figure 6, the intensity at 1725 cm^{-1} decreases with temperature. This phenomenon can be attributed to the thermal-induced decomposition of carbonate group in the polymer. Based on the prediction of Figure 5, the mass loss from 140 to 300℃ can sum up about 75%. Although the FTIR spectra of resists B and C are not shown here, they exhibit the same vibration tendency against temperature with resist A.

3.3 Effect of Copolymer Modification on Process Performance for Electron Beam Resist

The resists, namely A, B and C, are underwent the etching with the fluorine-containing plasma to evaluate the etching durability of modification with poly(styrene-co-maleic anhydride) copolymer. It is interestingly found from Table 3 that the resist after 1 and 2% w/v copolymer modification can significantly improve the etching resistance. What is the reason for this behavior? According to the finding of GPC method in previous section, the molecular weight distribution for resists A, B and C is still unchangeable except the 1824 Da. This observation indicates the spiking copolymer can not polymerize with the original resist polymer appeared in Figure 3, poly(α-chloro-acrylate-co-α-methylstyrene). Therefore, the achieving of higher etching resistance for resists B and C is not due to the elevation of molecular weight.

Shibata and coworkers[21] used the model of fullerence-incorporated positive electron beam resist to explain the improvement of etching resistance. Namatsu et al.[19] proposed the edge roughness of resist pattern was caused by polymer aggregation. Together with the above two reports, the possible configuration between resist A and the spiking copolymer is depicted in Figure 7. Owing to the chain aggregation of main resist polymer after baking, the vacancy is found in the resist A. The spiking copolymer chain can also aggregate in the form of small bead during baking. The vacancy appeared in resist A can be filled with the small bead, and therefore, the film becomes more densification. This observation increases the etching tolerance for the modified resist. In addition, Table 3 also indicates the etching resistance is increased with the spiking amount. This result is due to the fact that large portion of vacancy during polymer of resist A can be filled with small bead. Hence, the plasma gas can not penetrate deeper to promote the etching rate.

The etching performance can be achieved by polymer modification, while the lithographic performance such as sensitivity and resolution remain to be evaluated. Figure 8 illustrates the sensitivity curve and SEM picture for resists A and B, the thickness of the resist layer decreases with the imposing dose. The experimental results also demonstrate the sensitivity, contrast and dose-to-clear are in the same, regardless of copolymer modification. This finding confirms the copolymer modification is the feasible mean to improve the etching resistance without adverse effect on lithographic behavior.

3.4 The Effect of Plasma Etching and Ion Implantation on Resist Stripping

The final step in the lithographic processing is resist stripping. In our laboratory, the standard resist stripping for front-end-of-line is first ozone ashing, and then cleaning with the mixture of sulfuric acid and hydrogen peroxide. In this study, the stripping effect of resists A and C after plasma etching and ion implantation is evaluated with the novel TDS-APIMS method. The TDS-APIMS method can determined the amount of surface organic at different desorption temperature.

Figure 9a and 9b illustrate the mass spectra of resists A and C without plasma etching and ion implantation. It can be found from TDS-APIMS spectra that the resist C has lower peak intensity than resist A. This observation indicates the resist modification can facilitate the resist stripping.

Downloaded From: http://proceedings.spiedigitallibrary.org/ on 04/28/2014 Terms of Use: http://spiedl.org/terms

Figure 10a and 10b illustrate mass spectra for resists A and C after plasma etching. It indicates the residual organic for resists A and C is similar. As compared with Figure 9, the surface organic after plasma etching and resist stripping is lower. This finding indicates the plasma etching has no adverse effect on resist stripping. On the contrary, the plasma etching is beneficial for the surface in the cleaning state.

Figure 11a and 11b illustrate the mass spectra for resist A and C after ion implantation. It is interestingly found that the resist A has more organic residue on the surface than resist C. In addition, the resists after ion implantation also facilitate the surface cleaning.

It has been reported that the plasma etching and ion implantation can degrade the stripping behavior. However, our results indicate the plasma etching and ion implantation can help the wafer surface to avoid organic contamination. Also, the copolymer modification is an effective mean to avoid surface organic contamination. This may be attributed to the interaction force between the resist and substrate. The aggregation model proposed in Figure 7 clearly indicates resist A possesses the more number of big bead in adhesion with the substrate. The interaction force between big bead and the substrate is higher than the small bead. As a consequence, the resist C, with few adhesion for big bead, shows the superior stripping behavior than resist A.

4. CONCLUSIONS

In this work, we have studied the molecular weight distribution and viscosity of modified resist, of which spiking with poly(styrene-co-maleic anhydride) copolymer. The spiking copolymer has no interaction and/or reaction with the original resist. The thickness of the modified resist film is higher due to the increasing viscosity after modification. The thermal stability of the resist, as evaluated by the first derivative of the TGA curve and the FTIR method, shows there are two main decomposition regions. The carbonate group in the resist is thermal unstable since 140℃. The modification is an effective mean to improve the etching resistance for the electron beam resist. The polymer aggregation with different sizes of beads can be used to explain the etching durability. Owing to no interaction between modifier and resist, the sensitivity, contrast and resolution of the resists are still in the same. It is interestingly found that the modification is beneficial for the resist stripping. The plasma etching and ion implantation can not degrade the stripping effect.

ACKNOWLEDGMENTS

The authors would like to thank the National Science Council of Taiwan, R.O.C., for supporting this research through contract #NSC89-2721-2317-200. They also thank Dr. S.-L. Chen and Mr. M.-J. Liu for helping GPC experiment at Taiwan Semiconductor Manufacturing Company.

REFERENCES

1. C. Y. Chang and S. M. Sze, *ULSI Technology*, McGRAW-HILL, NY, 1996.
2. S. R. J. Brueck, and X. L. Chen, *J. Vac. Sci. Technol.*, **B17**, pp. 908, 1999.
3. M. Takahashi, S. Kishimura, T. Ohfuji, and M. Sasago, *Jpn. J. Appl. Phys.*, **37**, pp. 6723, 1998.
4. S. Mori, K. Kuhara, T. Morisawa, N. Matsuzawa, Y. Kaimoto, M. Endo, T. Matsuo and M. Sasago, *Jpn. J. Appl. Phys.*, **37**, pp. 6734, 1998.
5. D. L. White and O. R. Wood, *J. Vac. Sci. Technol.*, **B16**, pp. 3411, 1998.
6. J. F. Chen, T. Laidig, K. E. Wampler and R. Caldwell, *J. Vac. Sci. Technol.*, **B15**, pp. 2426, 1997.
7. C. C. Hsia, T.-S. Gau, C.-H. Yang, R.-G. Liu, C.-H. Chang, L.-J. Chen, C.-M. Wang, J.-F. Chen, B. W. Smith, G.-W. Hwang, J.-W. Lay and D.-Y. Goang, *Proc. SPIE*, **3679**, pp.427, 1999.
8. A. Schiltz, J. F. Terpan, G. Amblard and P. J. Paniez, *Microelec. Eng.*, **35**, pp. 221, 1997.
9. K. Elian, W. D. Domke, E. Gunther and M. Irmscher, *Microelec. Eng.*, **45**, pp. 319, 1999.
10. A. Blakeney, A. Gabor, D. White, T. Steinhausler, W. Deady, J. Jarmalowicz, R. Kunz, K. Dean, G. Rich and D. Stark, *Solid State Technol.*, **41**, pp. 69, 1998.
11. Thompson, L. F., Willson, C. G., and Bowden, M. J., *Introduction to Microlithography*, 2nd Ed., ACS, Washington, 1994, Chapter 2.
12. Nonogaki, S., Ueno, T., and Ito, T., *Microlithography Foundamentals in Semiconductor Devices and Fabrication Technology*, Marcel Dekker, New York, 1998, Chapter 7.
13. Y. Someda, Y. Shoda and N. Saitou, *J. Vac. Sci. Technol.*, **B14**, pp. 3742, 1996.
14. P. Jedrasik, *Microelec. Eng.*, **30**, pp.161, 1996.
15. H. Tomozawa, Y. Saida, Y. Ikenoue, F. Murai, Y. Suzuki, T. Tawa and Y. Ohta, *J. Photopolymer Sci. Technol.*, **9**, pp. 707, 1996.

Downloaded From: http://proceedings.spiedigitallibrary.org/ on 04/28/2014 Terms of Use: http://spiedl.org/terms

16. I. Ishii, H. Nozawa and T. Tamamura, *Appl. Phys. Lett.*, **70**, pp. 1110, 1997.
17. L. E. Ocola, C. J. Biddick, D. M. Tennant, W. K. Waskiewicz and A. E. Novembre, *J. Vac. Sci. Technol.*, **B16**, pp. 3705, 1998.
18. H. Namatsu, M. Nagase, K. Kurihara, K. Iwadate, T. Furuta and K. Murase, *J. Vac. Sci. Technol.*, **B13**, pp. 1473, 1995.
19. H. Namatsu, M. Nagase, T. Yamaguchi, K. Yamazaki and K. Kurihara, *J. Vac. Sci. Technol.*, **B16**, pp. 3315, 1998.
20. F.-H. Ko, J.-K. Lu, T.-C. Chu, T.-Y. Huang, C.-C. Yang, J.-T. Sheu and H.-L. Huang, *Proc. SPIE*, **3678**, pp. 429, 1999.
21. T. Shibata, T. Ishill, H. Nozawa and T. Tamamura, *Jpn. J. Appl. Phys.*, **36**, pp. 7642, 1997.

Table 1. Operating conditions for the reactive ion etcher

	step 1	step 2
pressure, torr	0.8	0.8
RF power, W	0	250
gas flow rate, cm^3/min		
Ar	1000	1000
O_2	20	20
CF_4	50	50
etching duration, sec	60	30

Table 2. The decomposition temperature (T_d) and the percentage of mass losses for the resists

Resist	first region		second region		residual mass (>600℃)
	T_d(℃)	%	T_d(℃)	%	%
A	280	94.1	544	4.0	0.87
B	278	94.0	547	2.8	0.59
C	306	94.0	551	2.8	0.71

Table 3. Etching resistance for the resists

Resist	etching resistance (nm/min)
A	582
B	241
C	221

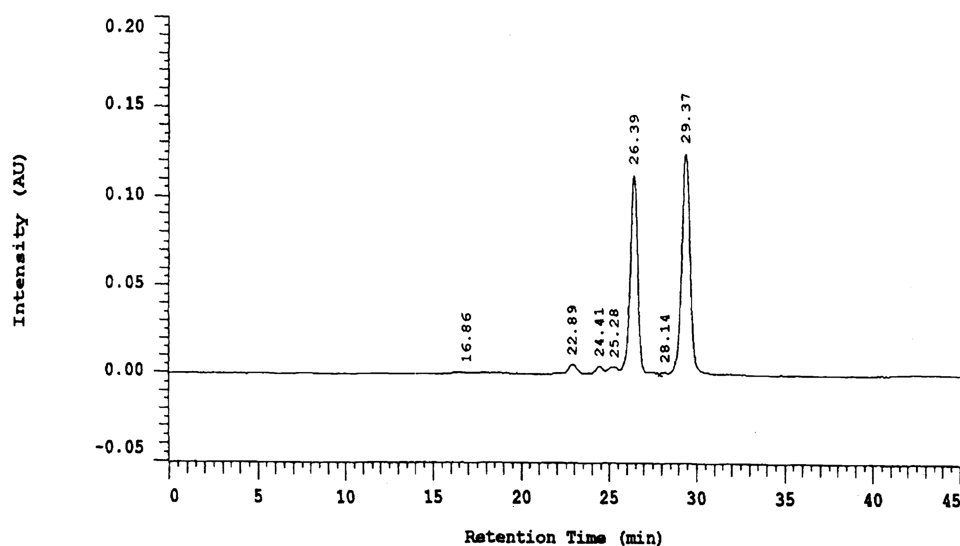

Figure 1. The chromatogram of resist C by eluting with GPC method.

Downloaded From: http://proceedings.spiedigitallibrary.org/ on 04/28/2014 Terms of Use: http://spiedl.org/terms

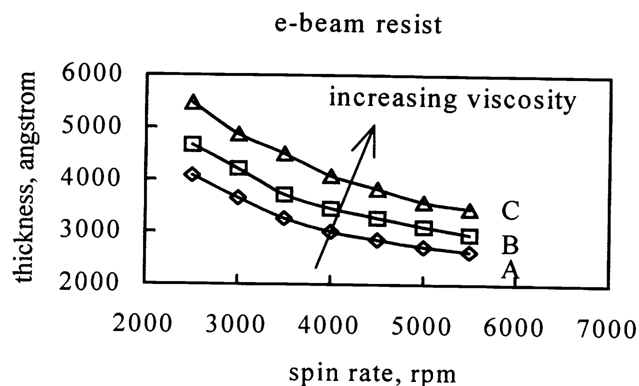

Figure 2. The effect of spin rate on resist film thickness.

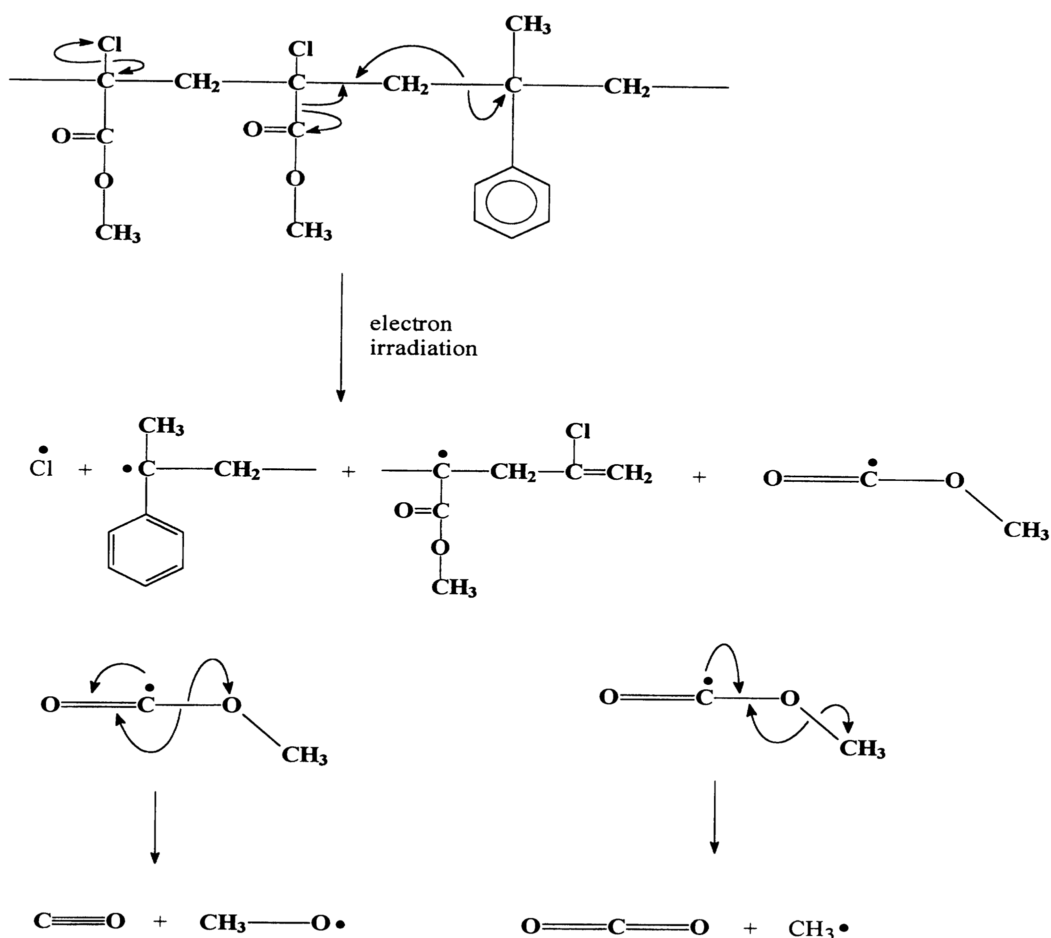

Figure 3. The reaction mechanism of electron irradiation on ZEP520 resist.

Downloaded From: http://proceedings.spiedigitallibrary.org/ on 04/28/2014 Terms of Use: http://spiedl.org/terms

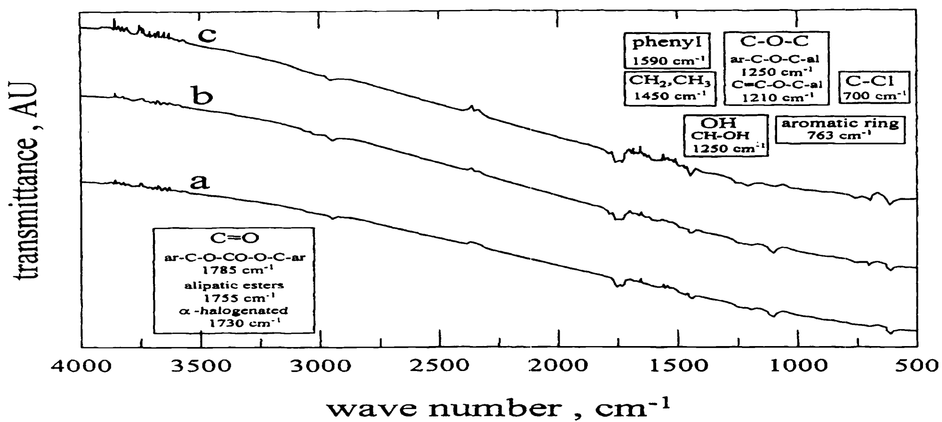

Figure 4. FTIR spectra for resists; lines a, b and c represent resists A, B and C.

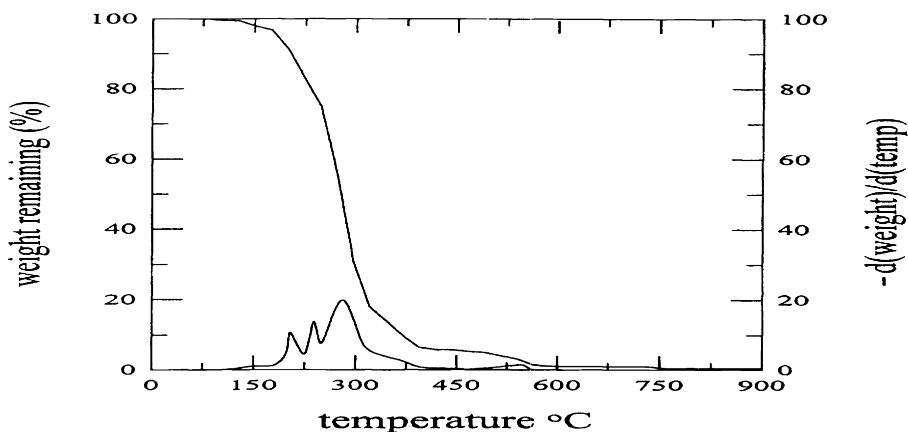

Figure 5. The effect of baking temperature on the mass change and the derivative TGA curve.

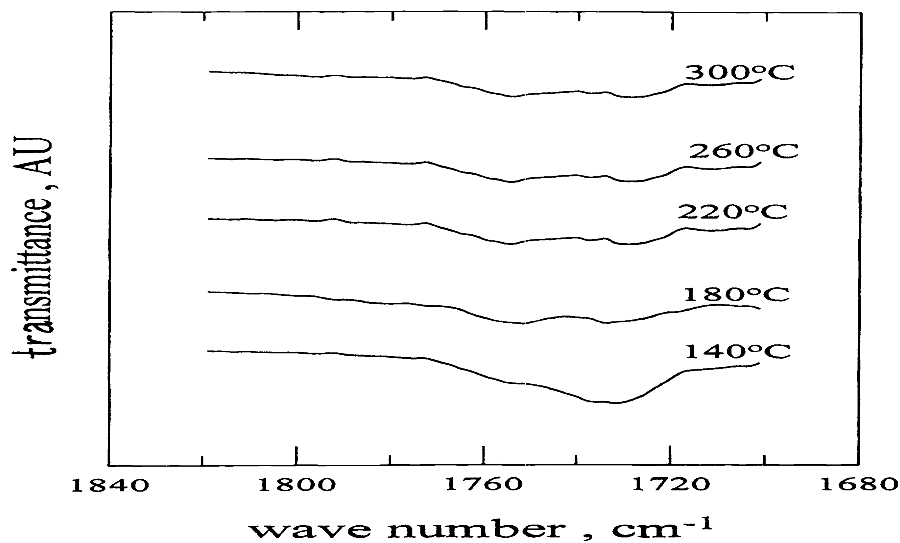

Figure 6. The FTIR spectra of resist A after various baking temperatures.

Downloaded From: http://proceedings.spiedigitallibrary.org/ on 04/28/2014 Terms of Use: http://spiedl.org/terms

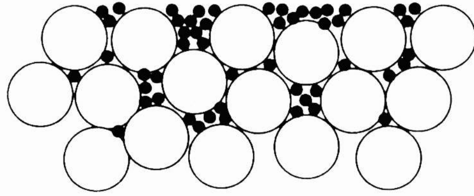

Figure 7. The aggregation model of polymer chain after baking. The open circle represents the original resist polymer (MW is about 54000 Da), and the solid circle represents the spiking polymer (MW is about 1900 Da).

8(a)

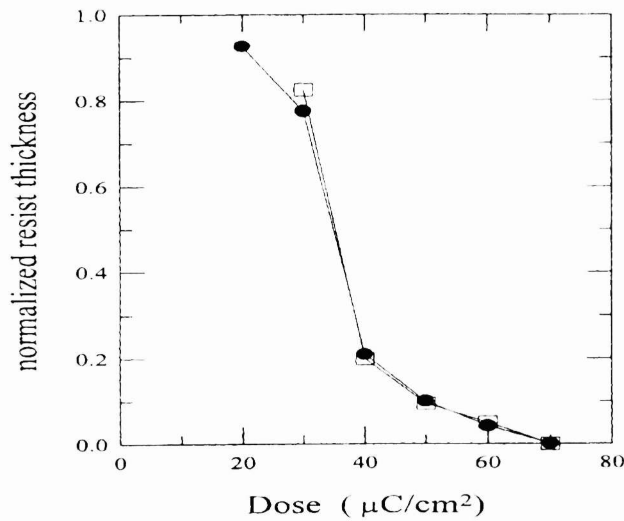

8(b)

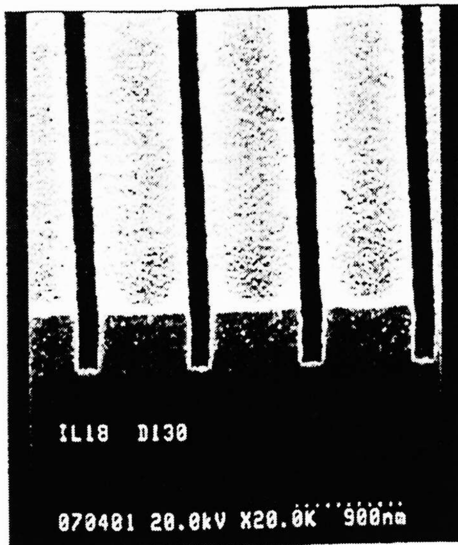

8(c)

Figure 8. (a) Sensitivity curve for resist A (solid circle) and resist B (open square); (b) SEM picture of 0.18μm trench for resist A; (c) SEM picture of 0.18μm trench for resist B.

Downloaded From: http://proceedings.spiedigitallibrary.org/ on 04/28/2014 Terms of Use: http://spiedl.org/terms

9(a)

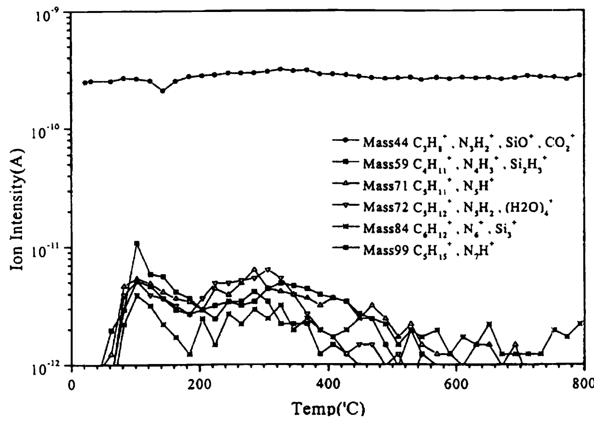

9(b)

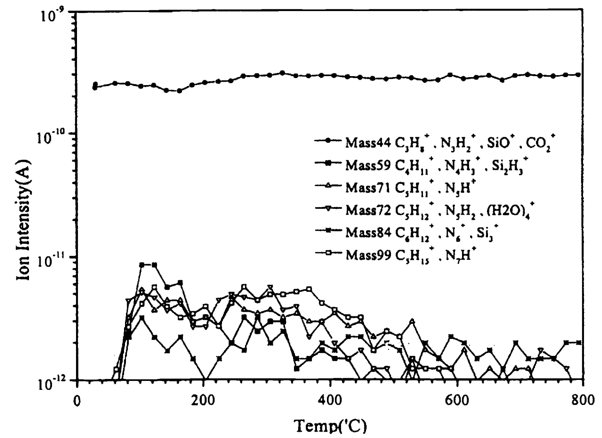

Figure 9. TDS-APIMS spectra for films of (a) resist A, and (b) resist C.

10(a)

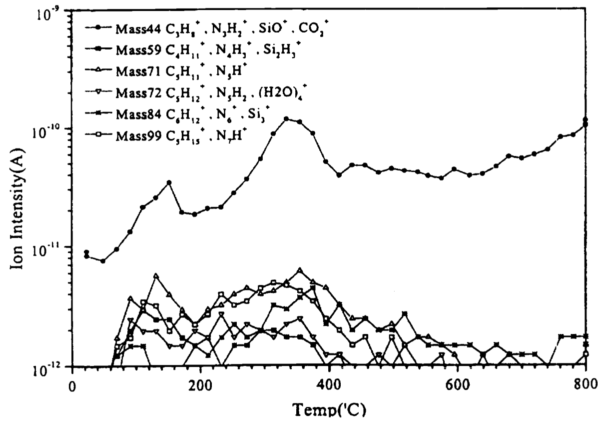

10(b)

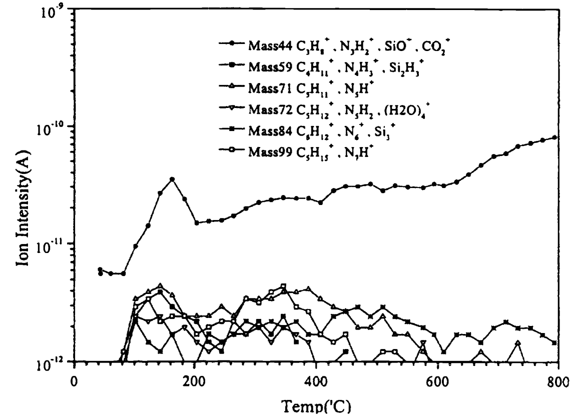

Figure 10. TDS-APIMS spectra for films of (a) resist A, and (b) resist C after plasma etching.

11(a)

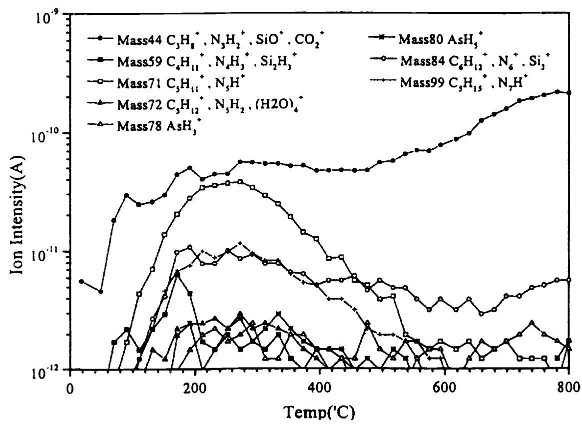

11(b)

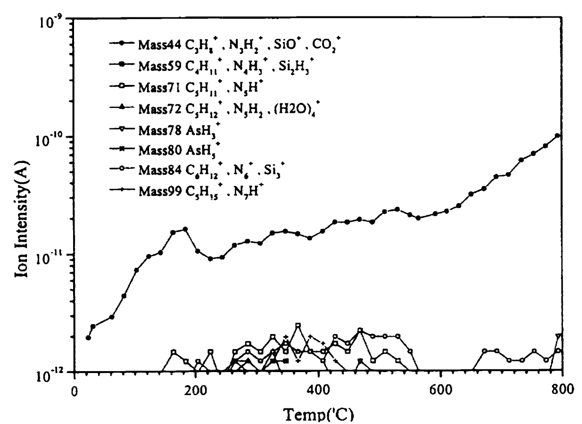

Figure 11. TDS-APIMS spectra for films of (a) resist A, and (b) resist C after ion implantation.

Downloaded From: http://proceedings.spiedigitallibrary.org/ on 04/28/2014 Terms of Use: http://spiedl.org/terms